Dynamics of the cantilever in noncontact dynamic force microscopy: The steady-state approximation and beyond

M. Gauthier,[1] N. Sasaki,[2,3] and M. Tsukada[1]
[1]*Department of Physics, Graduate School of Science, University of Tokyo, Hongo 7-3-1, Bunkyo-ku, Tokyo 113-0033, Japan*
[2]*Department of Materials Engineering, Graduate School of Engineering, University of Tokyo, Hongo 7-3-1, Bunkyo-ku, Tokyo 113-8656, Japan*
[3]*Core Research for Evolutional Science and Technology (CREST), Japan Science and Technology Corporation (JST), 2-1-6 Sengen, Tsukuba, Ibaraki 305-0047, Japan*
(Received 9 March 2001; published 3 August 2001)

A detailed analysis of models that have been used for describing the dynamics of the cantilever in large-amplitude noncontact dynamic force microscopy is presented. For each model, attention is especially paid to the nonlinear nature of the problem and its implication for experiments. In particular, in the steady-state approximation where the equations of motion for an externally and self-driven oscillator are rigorously identical, the theory predicts the existence of unstable solutions whether the interaction force is dissipative or not. The need to go beyond the steady-state approximation by including the finite-time response of the system to a change of tip-surface separation or interaction during the scanning is also discussed.

DOI: 10.1103/PhysRevB.64.085409 PACS number(s): 68.37.Ef, 07.79.Lh, 87.64.Dz

I. INTRODUCTION

Noncontact dynamic force microscopy (DFM) (Refs. 1–4) is a powerful tool for investigating various surfaces at an atomic scale. In experiments, the shift of the resonant frequency of the cantilever, which serves as a frequency determining element, is used for regulating the tip-surface separation. It is also possible to obtain additional atomic-scale information by simultaneously measuring the damping of the lever oscillation due to the surface[5–10] [these experiments have been performed with phase lock loop (PLL) techniques]. The damping can straightforwardly be interpreted as dissipation if the oscillator behaves linearly. However, in general, the cantilever is operated with large amplitude compared to the range of the tip-surface nonlinear potential, and it is yet not clear to what extent the problem remains linear. In interpreting surface images, it is therefore important to understand the dynamics of the cantilever before asserting what the apparatus is actually measuring. Most of the analytical works on the dynamics of the lever have focused on describing the steady-state solutions of the cantilever equation of motion.[11–15] In this approximation, quantities such as the amplitude, driving frequency, or excitation amplitude are treated as parameters. Unfortunately, the stability of the solutions, which is understood,[12,14] has only been briefly described and the implication of unstable solutions for real experiments has not been emphasized enough. Moreover, stability has not been discussed when including dissipation to the surface. Consequently, the validity of the steady-state approximation has never been seriously challenged. Not included in this approximation is the effect of the time dependence of the quantities mentioned above in actual experiments and the fact that time-averaged observables, such as the peak-to-peak oscillation amplitude,[16] are involved in the electronics.

In this paper, we analyze in detail the models that have been used for describing the dynamics of the lever. Attention is paid to the nonlinear features of the solutions. For instance, in the steady-state approximation where the equations of motion for an externally driven and self-driven oscillator are rigorously identical, the existence of unstable solutions is an unavoidable consequence of the nonlinearity of the interaction. This is also true when including the effects of dissipation to the surface on the lever of the dynamics. The failure to systematically observe mechanical instabilities and to reproduce the order of magnitude of the atomic scale corrugation of the damping signal (assuming it results from dissipation) based on first-principles theory and the fact that quantities such as the driving frequency and excitation amplitude are dynamically determined indicate the need to go beyond the steady-state approximation by including the finite-time response of the system to a change of separation or interaction.

II. STEADY-STATE APPROXIMATION

A. Weakly nonlinear integrable Hamiltonian

The theoretical description of DFM operated with large amplitude was begun with the work of Giessibl.[17] The Hamiltonian is

$$H = m\dot{x}^2/2 + kx^2/2 + U_i(x+L;X;Y), \tag{1}$$

where L is the mean tip-surface separation, k the cantilever effective spring constant, and U_i the nonlinear potential. X and Y are the lateral coordinates of the tip. The equation of motion can be written as a set of first-order differential equations referred to as a flow:

$$\begin{pmatrix} \dot{y} \\ \dot{x} \end{pmatrix} = \begin{pmatrix} -\omega_0^2 x + F_i(x+L)/m \\ y \end{pmatrix}, \tag{2}$$

with $\omega_0^2 = (2\pi f_0)^2 = k/m$. The flow is two dimensional and autonomous (no explicit time dependence). Because the nonlinear potential $|U_i|$ is much smaller than $kx^2/2$, the system is only weakly nonlinear. One can therefore use first-order

perturbation theory[17] or Fourier analysis for obtaining an expression for the cantilever resonant frequency shift,

$$\Delta f_{\mathrm{NIH}} = -\frac{f_0}{2} r(A,L), \tag{3}$$

where $r(A,L)$ is some unitless average of the interaction force over one oscillation period,

$$r(A,L) \equiv \frac{1}{kA\pi} \int_0^{2\pi} F_i(A\cos\theta + L)\cos\theta \, d\theta. \tag{4}$$

The dependence of the frequency shift, Eq. (3), on the oscillation amplitude A and its order of magnitude agree well with various experiments (see, e.g., Ref. 8). Note that within this model, the atomic-scale damping is not related to the dynamics of the cantilever. Following the work of Giessibl, Eq. (1) has also been used as a starting point by a number of authors.[18–24]

B. Inclusion of an intrinsic dissipative and forcing term

The treatment can easily be extended by including intrinsic dissipation and forcing. The equation of motion can have many variations depending on the specific model used for the driving term. Here two models are discussed: the so-called externally driven oscillator

$$\ddot{x} + \frac{\omega_0}{Q_0}\dot{x} + \omega_0^2 x = F_i(x+L)/m + A_{\mathrm{d}}\omega_0^2 \cos(\omega t) \tag{5}$$

and the self-driven oscillator

$$m\ddot{x} + \frac{\omega_0 m}{Q_0}\dot{x} + kx = F_i(x+L) + Gkx(t-t_0). \tag{6}$$

A_{d}, G, t_0, and Q_0 are the excitation amplitude, gain factor, time delay, and intrinsic quality factor, respectively. Equation (5) describes PLL electronics. The driving term is exactly sinusoidal because it is the voltage-controlled oscillator (VCO) output signal.[25] Equation (6) describes an experimental setup with an automatic gain control (AGC) where the time-delayed cantilever signal is used to excite the cantilever.[1,16] Here A_{d} and ω [Eq. (5)], or G (Ref. 16) and t_0 [Eq. (6)] can be complicated functions of time for describing real electronics. Within the steady-state approximation, however, they are treated as parameters because one seeks steady-state solutions of the form $x(t) = A\cos(\omega t - \phi)$ for Eq. (5) or $x(t) = A\cos(\omega t)$ for Eq. (6). The main difference with the previous case is that these equations are no longer autonomous [in Eq. (6), $x(t-t_0)$ cannot be expressed in terms of $x(t)$]. Equivalently, Eq. (5) can be written as a three-dimensional autonomous flow,

$$\begin{pmatrix} \dot{y} \\ \dot{x} \\ \dot{\xi} \end{pmatrix} = \begin{pmatrix} -\frac{\omega_0}{Q_0} y - \omega_0^2 x + F_i(x+L)/m + A_{\mathrm{d}}\omega_0^2 \cos(\omega\xi) \\ y \\ 1 \end{pmatrix}, \tag{7}$$

and similarly for Eq. (6). Here $\{L, A, \phi, A_{\mathrm{d}}, \omega, X, Y\}$ and $\{L, A, t_0, G, \omega, X, Y\}$ span a seven-dimensional parameter space for an externally and self-driven oscillator, respectively. It is easy to demonstrate that the equation of motion for an externally driven and self-driven oscillator are rigorously identical within this approximation. One simply needs to insert the ansatz for $x(t)$ into Eq. (6), make the change of variable $t - t_0 \to t$, and the assignments $\phi = 2\pi - \omega t_0$ (assuming $\pi \leqslant \omega t_0 \leqslant 2\pi$) and $G = A_{\mathrm{d}}/A$. Physically, these are equivalent because, for a steady-state, the causality relationship has the property that there is no distinction between the lever responding to a periodic external excitation or the lever exciting itself with a time delay. The equivalence of these models in the steady state approximation has motivated many authors[11–15,26] to use the equation of motion of an externally driven oscillator for successfully studying DFM. Note the striking resemblance between Eq. (5) and the well-studied Duffing equation[27] with a small anharmonic perturbation.

The effective potential energy $U_i(x+L) + kx^2/2$ is obviously asymmetric around $x = 0$. Although this may naively be thought to imply an anharmonic cantilever motion, this is not the case since, as pointed out above, the magnitude of F_i is much smaller than $|kx|$.[24] In the tapping mode, the cantilever motion is still sinusoidal for soft enough surfaces even though the magnitude of the interaction is usually significantly larger.[28–30] An explicit evaluation of the importance of anharmonicity in DFM based on Fourier analysis is presented in the Appendix. While Fourier analysis can be used for obtaining the solutions of the equation of motion, it does not provide information on their stability. One must have recourse to the theory of nonlinear differential equations[27] for this purpose. The fixed points, corresponding to the steady-state solutions, can be determined by using the time averaging and perturbation approach or Poincaré map. The idea is to reduce the flow, Eq. (7), to an averaged two-dimensional autonomous one [the sign of ϕ is determined by the form of the ansatz $x = A\cos(\omega t - \phi)$]:

$$\begin{pmatrix} \dot{A} \\ A\dot{\phi} \end{pmatrix} = \frac{1}{2\omega} \begin{pmatrix} -\omega\omega_0 A/Q_0 + A_{\mathrm{d}}\omega_0^2 \sin\phi \\ (\omega^2 - \omega_0^2)A + A_{\mathrm{d}}\omega_0^2 \cos\phi + A\omega_0^2 r(A,L) \end{pmatrix}. \tag{8}$$

The fixed points are obtained by fixing $\dot{A}$ and $A\dot{\phi}$ to zero. This leads to the following equations of the steady-state approximation:

$$\frac{A_{\mathrm{d}}}{A}\cos\phi = \frac{\omega_0^2 - \omega^2}{\omega_0^2} - r(A,L) \tag{9}$$

and

$$\frac{A_{\mathrm{d}}}{A}\sin\phi = \frac{1}{Q_0}. \tag{10}$$

Equations (9) and (10) (Refs. 12 and 14) define a hypersurface $\mathcal{H}$ in the seven-dimensional parameter space. In the steady-state approximation, this hypersurface describes all possible solutions of the equation of motion Eq. (5) or Eq.

(6). The local stability of a given fixed point is determined by linearizing the flow in its vicinity and finding the eigenvalues. The secular equation is (λ represents the eigenvalues)

$$\lambda^2+\left(\frac{\omega\omega_0}{Q_0}+\frac{A_d\omega_0^2\sin\phi}{A}\right)\lambda+\{\omega_o^2[1-g(A,L)]-\omega^2\}\times\frac{A_d}{A}\omega_0^2\cos\phi+\frac{\omega\omega_0}{Q_0}\frac{A_d}{A}\omega_0^2\sin\phi=0, \tag{11}$$

where $g(A,L)$, a quantity similar to $r(A,L)$, is defined as

$$g(A,L)\equiv\frac{1}{k\pi}\int_0^{2\pi}\frac{dF_i(A\cos\theta+L)}{dx}\cos^2\theta\,d\theta. \tag{12}$$

A steady-state solution is unstable if the condition

$$S\equiv\left(1-\frac{\omega^2}{\omega_0^2}-g(A,L)\right)\frac{A_d}{A}\cos\phi+\frac{1}{Q_0^2}<0 \tag{13}$$

is satisfied (i.e., $\lambda>0$), or else it is stable. In the following, S is referred to as the stability function. Equations (9), (10), and (13) provide all the information about the dynamics of the lever in the steady-state approximation for a conservative force.

A solution of particular interest is the one having a phase $\pi/2$. According to Eqs. (13) and (9), it is stable and corresponds to a frequency shift equal to $\Delta f_{\rm NIH}$.[12,14,15] Since this state has the maximum amplitude for a given A_d, it is naturally referred to as the resonant state. Therefore the introduction of intrinsic dissipation and driving does not alter the conclusion that $\Delta f=\Delta f_{\rm NIH}$ and the damping is unrelated to the dynamics of the cantilever.

It should be clearly understood that the hypersurface $\mathcal{H}$ defined by Eqs. (9) and (10) is an object whose properties are independent of the way it is sampled. In order to emphasize this point and demonstrate the relevance of unstable solutions for real experiments, the hypersurface $\mathcal{H}$ is projected onto four constant parameter hypersurfaces: $\{L,A_d,X,Y\}$, $\{\phi,A_d,X,Y\}$, $\{A,\phi,X,Y\}$, and $\{A,L,X,Y\}$. For the sake of illustration, the following constants are defined: $L^*=103.5$ Å, $A^*=100$ Å, $A_d^*=A^*/Q_0$ and $U_i(X^*;Y^*)$ is assumed to be a Morse potential,

$$U_i(x;X^*;Y^*)=U_0\left\{\left[1-\exp\left(-2b\frac{x-R_c}{R_c}\right)\right]\right\}, \tag{14}$$

with $U_0=2.273$ eV, $b=1.497$, and $R_c=2.357$ Å.[31] The force F_i is plotted in Fig. 1. The cantilever is characterized by $k=40$ N/m, $Q_0=10^4$, and $f_0=150$ kHz.

1. Constant parameter hypersurface $\{L^*,A_d^*,X^*,Y^*\}$

The intersection of the hypersurface $\mathcal{H}$ with this constant parameter hypersurface is shown in Figs. 2(a) and 2(b). It corresponds to a phase variation experiment with constant excitation. The shape of the curves are qualitatively very similar to that of the Duffing's problem.[27] The curves are extremely distorted (multivalued) around the solution $(A^*,\pi/2)$. The emergence of such distorted structures is an unavoidable consequence of large-amplitude operation even when the system is only weakly nonlinear (as is the case here). All solutions are stable except those corresponding to the lower part of the needle edge which are indicated by the dotted line. Solutions are unstable when the stability function S defined in Eq. (13) is smaller than zero, as shown in Fig. 2(c).

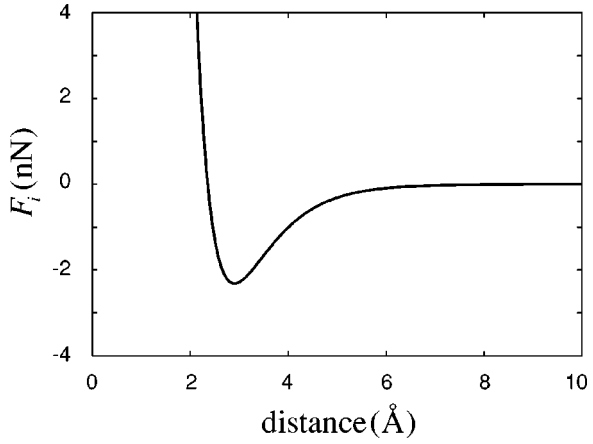

FIG. 1. Tip-surface interaction force used for the calculations. A Morse potential is assumed with parameters described in the text.

2. Constant parameter hypersurface $\{\phi^*,A_d^*,X^*,Y^*\}$

When the phase ϕ^* is fixed to $\pi/2$, all solutions have an amplitude A^* and are stable because $S=1/Q_0^2>0$. However, unstable solutions exist for phases $\phi^*\neq 90°$. Even for a small diminution of the phase—for example, when $\phi^*=89.5°$—unstable solutions emerge in the near-noncontact region as shown in Figs. 3(a) and 3(b). In Figs. 3(c) and 3(d), the phase is slightly larger than 90°—that is, $\phi^*=90.5°$—and the situation is reversed; some solutions in the contact region are unstable while all solutions in the noncontact region are stable.

Since DFM experiments are usually conducted with constant amplitude, the following constant parameter hypersurfaces are more directly of interest.

3. Constant parameter hypersurface $\{A^*,\phi^*,X^*,Y^*\}$

This projection corresponds to the normal operation for DFM. When $\phi^*=90°$, all solutions are stable independently of the separation L, as shown in Figs. 4(a) and 4(b). The situation is drastically different for phases $\phi^*\neq 90°$. For example, Figs. 4(c) and 4(d) show that for a phase $\phi^*=80°$, no stable solution is possible for some separation in the near-noncontact region. It is not difficult to see that if these unstable solutions were to be projected onto the constant parameter hypersurface similar to Fig. 2, they would be on the lower part of the needle edge. For a phase $\phi^*=100°$ [Fig. 4(e) and 4(f)], some solutions in the contact region become unstable and all others are stable.

4. Constant parameter hypersurface $\{A^*,L^*,X^*,Y^*\}$

This projection, shown in Fig. 5, corresponds to a phase variation experiment at constant amplitude. The nonlinear

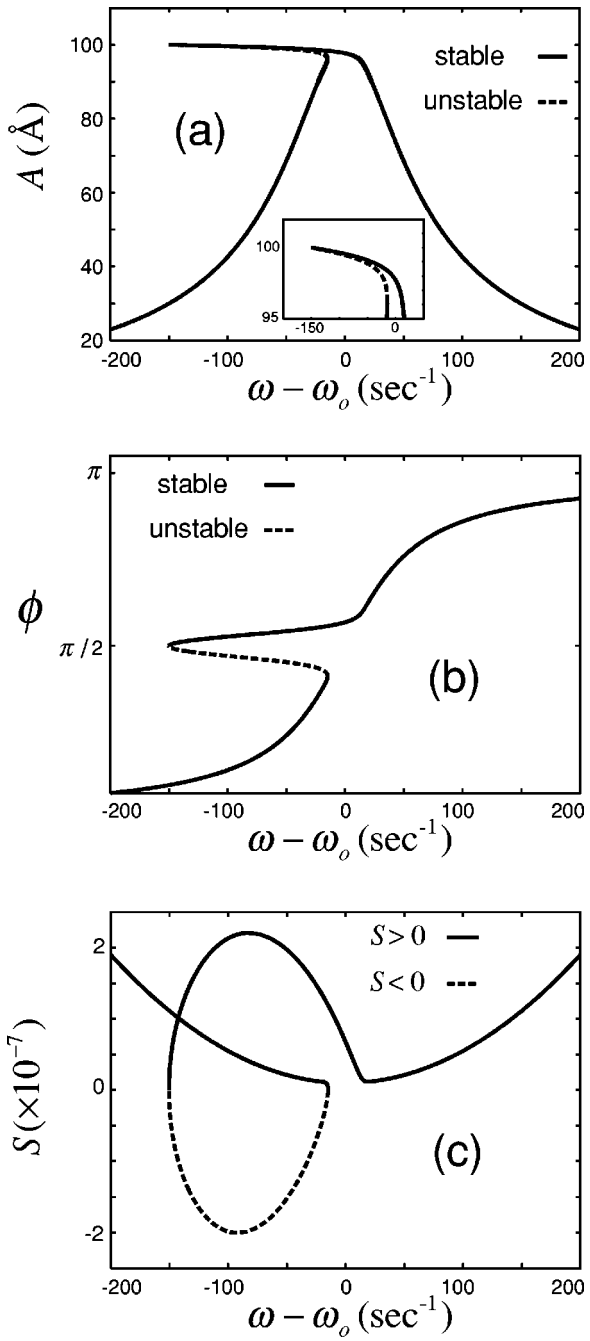

FIG. 2. Steady-state approximation: intersection of the hypersurface defined by Eqs. (9) and (10) with the constant parameter hypersurface $\{L^*, A_d^*, X^*, Y^*\}$. This corresponds to a phase variation experiment at constant excitation amplitude. (a), (b), and (c) show the amplitude, phase, and stability function, respectively. (a), (b) Extremely distorted structures around the solution ($A^* = 100$ Å, $\pi/2$) can be seen and unstable solutions exist because (c) S is not always positive. The general features are similar to the solutions of Duffing's equation with a small anharmonic perturbation.

nature is even more apparent; for phases smaller than $\pi/2$, there is no stable solution. Phase variation experiments at constant amplitude have been presented using PLL techniques and no instability was reported.[32]

As mentioned above, the expression for the frequency shift is identical to that found prior to the introduction of intrinsic dissipation and forcing. Even if the solution with $\phi = \pi/2$ is stable, it has been shown that many other solutions are not. Since the results presented in Figs. 4 and 5 are directly comparable with DFM experiments, the existence of instability can and should be verified experimentally. It is clear that the steady-state approximation is not satisfactory if these instabilities cannot be observed. As will be explained in the following section, instability should exist even when the effect of dissipation to the surface on the dynamics of the cantilever is included.

C. Inclusion of dissipation to the surface

So far, we have ignored the possibility that energy dissipates to the surface. For a dissipative interaction force $F_i(x;\dot{x})$, Eqs. (9), (10), and (13) generalize to

$$\frac{A_d}{A}\cos\phi = \frac{\omega_0^2 - \omega^2}{\omega_0^2} - r^+(A,L,\omega), \tag{15}$$

$$\frac{A_d}{A}\sin\phi = \frac{1}{Q_0} + r^-(A,L,\omega), \tag{16}$$

and

$$S \equiv \left(1 - \frac{\omega^2}{\omega_0^2} - g^+(A,L,\omega)\right)\frac{A_d}{A}\cos\phi + \left(\frac{1}{Q_0} + g^-(A,L,\omega)\right) \times \left(\frac{1}{Q_0} + r^-(A,L,\omega)\right) < 0, \tag{17}$$

respectively. The average functions r and g have been generalized to

$$r^{\pm}(A,L,\omega) \equiv \frac{1}{kA\pi}\int_0^{2\pi} F_i(A\cos\theta + L; -A\omega\sin\theta) \times \begin{Bmatrix}\cos\theta \\ \sin\theta\end{Bmatrix} d\theta \tag{18}$$

and

$$g^{\pm}(A,L,\omega) \equiv \frac{1}{k\pi}\int_0^{2\pi}\left(\frac{\partial F_i}{\partial x}\cos\theta - \frac{\partial F_i}{\partial \dot{x}}\omega\sin\theta\right) \times \begin{Bmatrix}\cos\theta \\ \sin\theta\end{Bmatrix} d\theta. \tag{19}$$

Equations (15) and (16) are equivalent to Eqs. (12) and (13) in Ref. 33. We immediately examine the nature of the frequency dependence of the function r^+. A dissipative term which is a separable function of x and $\dot{x}$ does not affect r^+. This is the case for the atomic-scale stochastic dissipation[34] $[\sim\gamma(x)\dot{x}]$ and dissipative currents for small-amplitude operation.[35] This is also the case for a piecewise continuous function of x in phase with $\dot{x}$ like phenomenological meta-

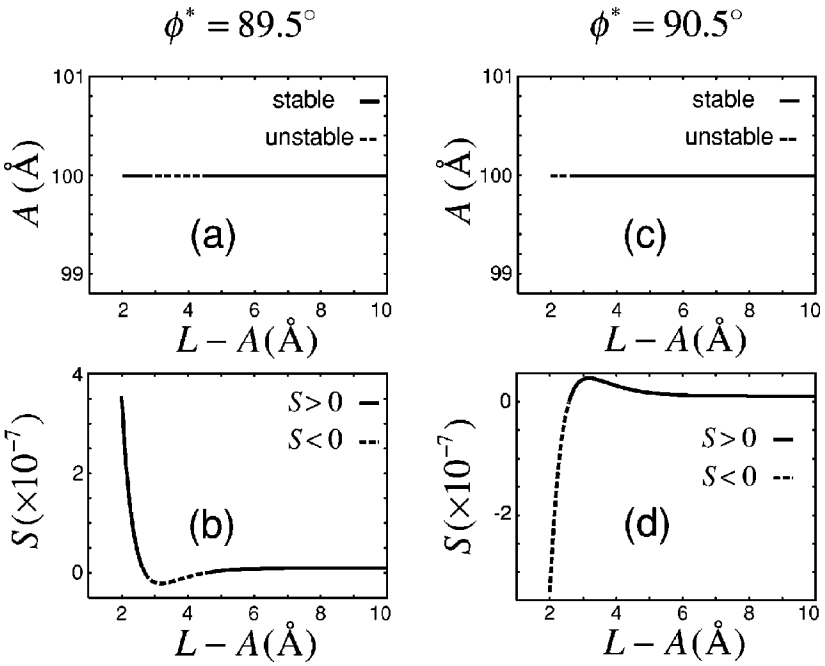

FIG. 3. Steady-state approximation: intersection of the hypersurface defined by Eqs. (9) and (10) with the constant parameter hypersurface $\{\phi^*, A_d^*, X^*, Y^*\}$. (a) and (c) [(b) and (d)] show the amplitude [stability function] at 89.5° and 90.5°, respectively. For a phase 90°, all solutions have an amplitude $A^* = 100$ Å and are stable since $S = 1/Q_0^2 > 0$ independently of the separation. (a), (b) However, even for a small diminution of the phase—for example, $\phi^* = 89.5°$—some solutions in the near-noncontact region become unstable since $S < 0$. (c), (d) Similarly, for a slight augmentation of the phase $\phi^* = 90.5°$, there are unstable solutions in the contact region.

stable stick-slip processes.[18,24,33] However, Loppacher *et al.*[8] have used a different model for the dissipative current; they used a retarded dissipative force of the form $F = \tilde{F}\cos(\omega t + \Delta\varphi)$ where $\tilde{F}$ and $\Delta\varphi$ are functions of ω. This leads to a term $\tilde{F}\cos\Delta\varphi/kA$ that contributes to r^+. Moreover, any adhesion hysteresis (i.e., stick-slip processes) which are not exactly in phase with the velocity but have some phase $\Delta\beta(\omega)$ could also account for the frequency dependence of r^+. It is illuminating to rewrite Eqs. (15) and (16) as

$$\tan\phi = [1/Q_0 + r^-(A,L,\omega)] \Big/ \left(\frac{\omega_0^2 - \omega^2}{\omega_0^2} - r^+(A,L,\omega) \right) \tag{20}$$

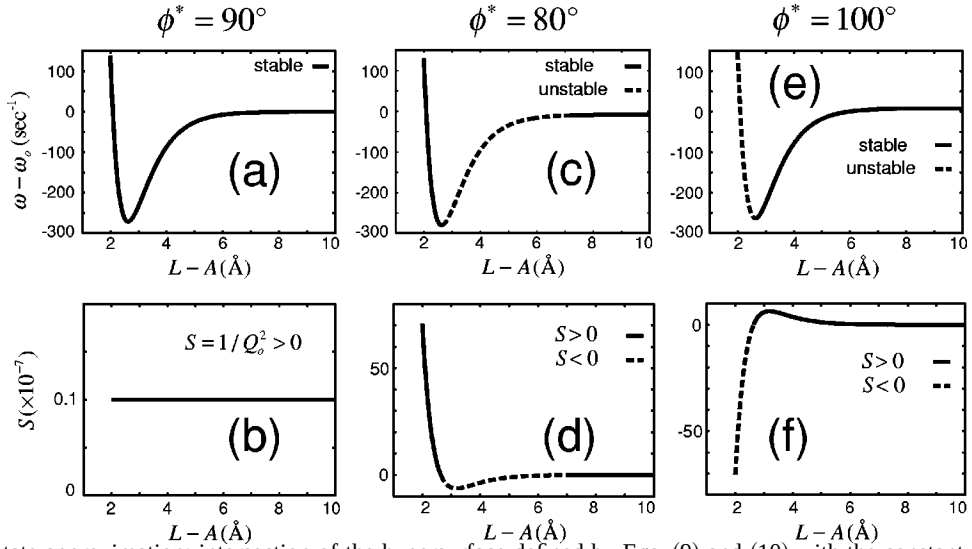

FIG. 4. Steady-state approximation: intersection of the hypersurface defined by Eqs. (9) and (10) with the constant parameter hypersurface $\{A^*, \phi^*, X^*, Y^*\}$. This corresponds to the normal DFM operation. (a), (c), and (e) [(b), (d), and (f)] show frequency shift profile [stability function S] at 90°, 80°, and 100°, respectively. (a) For a phase 90°, all solutions are stable because (b) S is always larger than zero. The situation is drastically different when the phase differs from 90°. (c), (d) When $\phi^* = 80°$, some solutions become unstable in the near-noncontact region; (e), (f) for $\phi^* = 100°$, some of the solutions in the contact region are unstable.

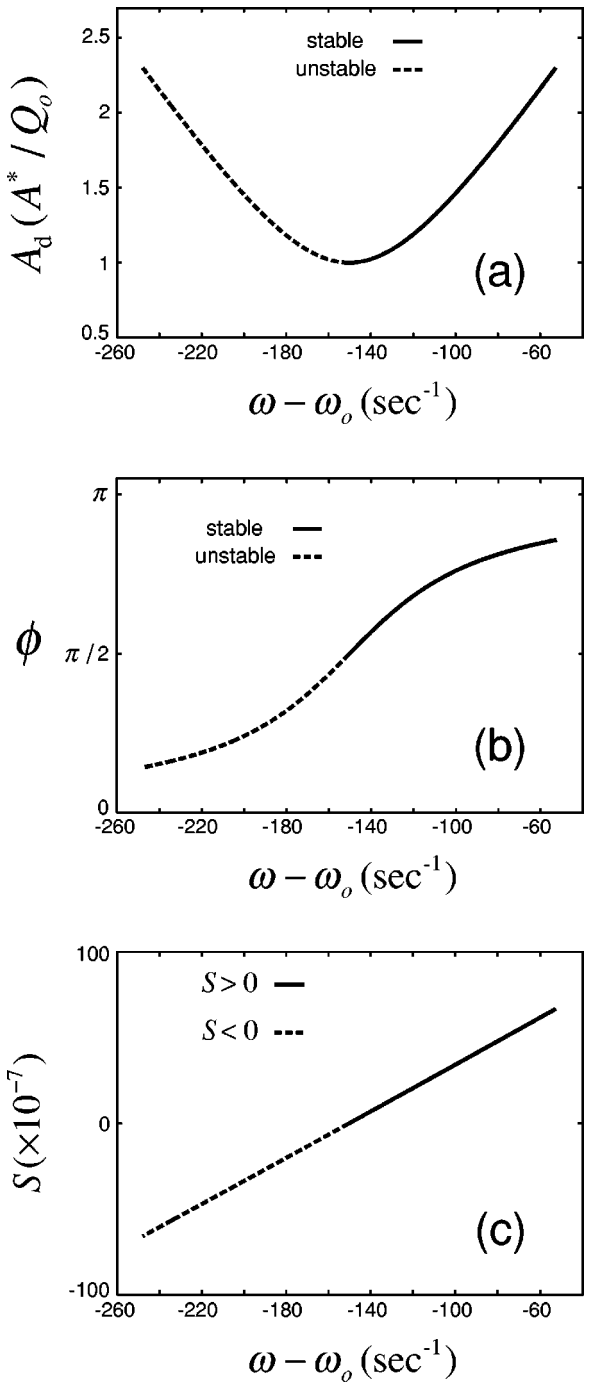

FIG. 5. Steady-state approximation: intersection of the hypersurface defined by Eqs. (9) and (10) with the constant parameter hypersurface $\{A^*,L^*,X^*,Y^*\}$. This corresponds to a phase variation experiment at constant amplitude. (a), (b), and (c) show the excitation curve, phase, and stability function S, respectively. For $\phi<\pi/2$, all solutions are unstable since $S<0$.

and

$$\frac{A_d}{A}=\sqrt{\left(\frac{\omega_0^2-\omega^2}{\omega_0^2}-r^+(A,L,\omega)\right)^2+[1/Q_0+r^-(A,L,\omega)]^2}. \tag{21}$$

According to Eq. (20), the dependence of r^+ on the frequency implies that dissipation affects the frequency of the solution corresponding to $\pi/2$:

$$\Delta f=-\frac{f_0}{2}r^+(A,L,f_0+\Delta f)\neq\Delta f_{\mathrm{NIH}}. \tag{22}$$

On the other hand, Eqs. (20) and (21) imply that this solution would not necessarily have the maximum amplitude because of the frequency dependence of r^-. For constant amplitude, the minimum excitation amplitude A_d occurs at the frequency ω_M given by

$$\left(\frac{\omega_0^2-\omega_M^2}{\omega_0^2}-r^+(A,L,\omega_M)\right)\left(\frac{2\omega_M}{\omega_0^2}+\left.\frac{\partial r^+}{\partial\omega}\right|_{\omega_M}\right)=\left(\frac{1}{Q_0}+r^-(A,L,\omega_M)\right)\left.\frac{\partial r^-}{\partial\omega}\right|_{\omega_M}. \tag{23}$$

The minimum of the excitation curve coincides with the phase $\pi/2$ only if $\partial r^-/\partial\omega=0$; otherwise, there is a phase shift ϕ_M:

$$\tan\phi_M=\left(\frac{2\omega_M}{\omega_0^2}+\left.\frac{\partial r^+}{\partial\omega}\right|_{\omega_M}\right)\Big/\left.\frac{\partial r^-}{\partial\omega}\right|_{\omega_M}. \tag{24}$$

It is emphasized that these frequency dependences are linked to slow dissipation processes but not to the atomic-scale stochastic dissipation[34] because the time scale of the motion of surface atoms is much smaller than that of the cantilever. It is worth noting that if the frequency dependence of the slow dissipation processes is roughly linear around ω_M, then Eq. (21) can be rewritten as $A_d(\omega_M+\delta\omega)/A\approx\sqrt{K_1(\delta\omega)^2+K_2}$, where $\delta\omega$ represents any departure from ω_M such that $\delta\omega\ll\omega_M$, and K_1, K_2 are constant. In other words, as long as the slow dissipation mechanisms are not very sensitive functions of the frequency, then the excitation curve should be approximately symmetrical around ω_M. In any case, these frequency dependences need to be more cautiously studied and are beyond the scope of this work.

Apart from these possible small frequency dependences, the physical origin of r^+ and r^- is very different (this is also true for g^+ and g^-). Here r^+ is essentially related to the average force over an oscillation period; r^- depends on the dissipation mechanism involved. It is thus unrealistic to assume that the average force and dissipation mechanism could ensure that the projection similar to that shown in Fig. 2 is always singled valued [i.e., the stability function S in Eq. (17) always larger than zero] for any separation L. In other words, unstable solutions should exist even when some dissipation to the surface takes place.

III. FULLY NONAUTONOMOUS TREATMENT

In real DFM experiments, A, ϕ, L, ω, X, Y, and A_d are not parameters but (time-dependent) variables. The fully nonautonomous three-dimensional flow is

$$\begin{pmatrix} \dot{y} \\ \dot{x} \\ \dot{\xi} \end{pmatrix} = \begin{pmatrix} -\frac{\omega_0}{Q_0} y - \omega_0^2 x + F_i(x+L(\xi);X(\xi);Y(\xi))/m + A_d(\xi)\omega_0^2 \cos[\omega(\xi)\xi] \\ y \\ 1 \end{pmatrix}; \tag{25}$$

a similar generalization holds for Eq. (6). It is urgent to clarify whether or not this extra nonautonomicity can alter the dynamics of the lever in DFM. The inclusion of the response of the system to a change of L, X, or Y could add extra structure to the global stable manifold of the periodic cycles. A step in this direction is found in Ref. 36 where it was argued that nonautonomous nonlinear effects (L was a variable) could contribute to the atomic-scale corrugation of the damping signal for PLL electronics (see, for example, Ref. 6) even though the cantilever motion is sinusoidal to a high degree of accuracy. Note that the simulations presented in Ref. 16 which aim at understanding a different type of electronics setup, do not show any departure from the steady-state approximation (the phase was always $\pi/2$).

There are a number of reasons to believe that the fully nonautonomous equation of motion needs to be considered. First, instabilities predicted in the steady-state approximation have not been observed experimentally. Second, the hypersurface $\mathcal{H}$ is extremely distorted around solutions with $\pi/2$, which can become unstable even for a small perturbation. On the other hand, it is well known that three-dimensional flows can lead to a practically infinite set of new phenomena (e.g., chaotic behavior).[27] This may not the case in the steady-state approximation because $\{L,A,\phi,A_d,\omega,X,Y\}$ are treated as parameters, which means that the system has in fact been assumed to respond *instantaneously* to any change in the separation or interaction. In real experiments, however, the response of the system is not instantaneous. For example, PLL electronics was reported to take ~ 1 ms to adjust its phase to an input signal phase step.[25] Also the electronics depends on time-averaged observables. For instance, the excitation or gain factor depends on the peak-to-peak oscillation amplitude which is a time-averaged quantity. Moreover, the sensitivity to a sudden change may be reduced because the feedback circuit depends on the history of such time-averaged observables [see, for example, Eq. (2) in Ref. 16].

Consider, for example, the case where the tip is initially located directly above one surface atom and a small change in X occurs (during the scanning). The situation is equivalent to a sudden small change in the interaction force (diminution). If the lever is oscillating at one of the fixed points with $\phi=\pi/2$ in the hypersurface $\mathcal{H}$ and if the response of the electronics is not instantaneous, then there is a chance that for some time the lever would be oscillating at a frequency below that of the new resonance, which may lead to substantially different dynamics.

Thus, these considerations in addition to the discussion presented in Ref. 36 for PLL electronics and the failure to observe instability experimentally may indicate that a proper treatment of the fully nonautonomous flow is essential for understanding the dynamics of the lever operated with large amplitude. We emphasize that the equations for an externally driven and self-driven oscillator are potentially different only within a fully nonautonomous treatment. In fact, there is no reason to believe that nonautonomous nonlinear effects, if any, should be the same since the equivalence between the two models only holds within the steady-state approximation. This may explain why different electronics setup can lead to different results.

IV. SUMMARY

In summary, in the steady-state approximation where the equations of motion for an externally and self-driven oscillator are rigorously identical, Eqs. (9), (10), and (13) [Eqs. (15), (16), and (17)] provide all information about the solutions for a conservative [dissipative] force. It is explained why instability is an unavoidable consequence of the nonlinear nature of the interaction for large-amplitude operation even when the interaction force is dissipative and how this could be verified experimentally. Because the solutions with $\phi=\pi/2$ are located in a very highly nonlinear region of the hypersurface and because in this approximation the response of the system is in fact assumed to be instantaneous, it is important to consider the dynamical problem in a fully nonautonomous way and to include the finite-time response of the system. We are currently working on extending our previous works in this direction. In parallel, effort should also be put into understanding atomic-scale dissipation mechanisms in DFM based on first-principles theory. An important and original proposal was recently made by Kantorovich for treating the stick-slip process as a nonequilibrium process.[37] In doing so he may be able to treat atomic-scale stochastic[34,38] and metastable stick-slip processes[33] within the same theoretical framework.

ACKNOWLEDGMENTS

This work was supported in part by a Grant-in-Aid on Priority Areas from the Ministry of Education, Science and Culture, Japan. M.G. acknowledges support from the Ministry of Education of Japan.

APPENDIX

The cantilever motion can be rigorously described by introducing the quantity δx representing the cantilever motion departure from purely sinusoidal,

$$x = x_0 + \delta x = A\cos(\omega t - \phi) + \delta x, \tag{A1}$$

where $\delta x \equiv \delta_0/2 + \Sigma_{n=2}^{\infty}\delta_n^+ \cos n(\omega t - \phi) + \Sigma_{n=2}^{\infty}\delta_n^- \sin n(\omega t - \phi)$. By Fourier expanding the interaction force F_i, the following can be obtained:

$$\tan\phi = \frac{\omega'/Q_0 + \delta r_2}{(1-\omega'^2) - (r_1 + \delta r_1)}, \tag{A2}$$

$$A'^2_{\mathrm{d}} = [(1-\omega'^2) - (r_1+\delta r_1)]^2 + [(\omega'/Q_0) + (\delta r_2)]^2, \tag{A3}$$

where $\omega' \equiv \omega/\omega_0$ and $A'_d \equiv A_d/A$. Here r_n is given by

$$r_n \equiv \frac{1}{kA\pi}\int_0^{2\pi} F_i(x_0+L)\cos n(\theta-\phi)\, d\theta, \tag{A4}$$

with $\theta \equiv \omega t$. Here δr_1, δr_2 represent corrections from first-harmonic motion. In the noncontact limit, δr_1, δr_2 can be written

$$\delta r_1 \approx \frac{\delta'_0}{2} g_{10}^+ + \sum_{l=2}^{\infty} g_{1l}^+ \delta'^+_l, \qquad \delta r_2 \approx \sum_{l=2}^{\infty} g_{1l}^- \delta'^-_l, \tag{A5}$$

with $g_{nl}^{\pm}$ defined as

$$g_{nl}^{\pm} \equiv \frac{1}{k\pi}\int_0^{2\pi} \left.\frac{dF_i}{dx}\right|_{x_0} \frac{1}{2}\{\cos[(l-n)(\theta-\phi)] \pm \cos[(l+n)(\theta-\phi)]\}\, d\theta. \tag{A6}$$

The coefficients $\delta'^{\pm}_n \equiv \delta_n^{\pm}/A$ can be determined by solving the following set of $2M-1$ linear equations, M representing the order of the highest harmonic included in the calculation:

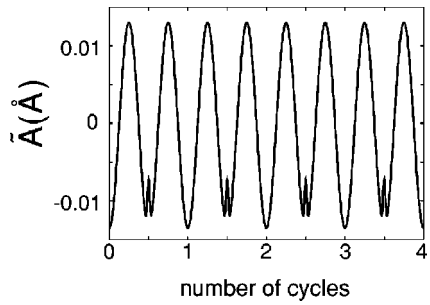

FIG. 6. Anharmonic effect. The quantity $\tilde{A}$ provides information on the importance of anharmonic effects in DFM. In the noncontact limit, $\tilde{A}$ can be calculated with the procedure explained above. $\tilde{A}$ differs from zero by at most ~ 0.015 Å at the separation $L^* = 103.5$ Å.

$$\left(1 - \frac{g_{00}^+}{2}\right)\delta'^+_0 - \sum_{l=2}^{M} g_{0l}^+ \delta'^+_l \approx r_0,$$

$$(1-n^2)\,\delta'^+_n + n/Q_0\,\delta'^-_n - g_{n0}^+\frac{\delta'^+_0}{2} - \sum_{l=2}^{M} g_{nl}^+ \delta'^+_l \approx r_n,$$

$$(1-n^2)\,\delta'^-_n - n/Q_0\,\delta'^+_n - \sum_{l=2}^{M} g_{nl}^- \delta'^-_l \approx 0. \tag{A7}$$

Roughly speaking, Eqs. (A5) and (A7) are accurate as long as $|\omega'-1| \ll 1$ and $|g_{00}^+|/2 \ll 1$. A useful quantity for measuring the deviation from purely sinusoidal is $\tilde{A} \equiv \sqrt{x^2 + (\dot{x}/\omega)^2} - A$. This is plotted in Fig. 6 for the force described in the text at $L^* = 103.5$ Å. The quantity $\tilde{A}$ departs from zero by at most ~ 0.015 Å. Apart from the introduction of the driving term, these considerations are similar to those discussed by Dürig in Ref. 24. Here we emphasize the following. In the noncontact region, Eq. (A7) provides a very simple way to calculate accurately the anharmonic terms; one simply has to solve a set of linear equations.

[1] T. R. Albrecht, P. Grütter, D. Horne, and D. Rugar, J. Appl. Phys. **69**, 668 (1991).
[2] F. J. Giessibl, Science **267**, 68 (1995).
[3] S. Kitamura and M. Iwatsuki, Jpn. J. Appl. Phys., Part 2 **34**, L145 (1995).
[4] H. Ueyama, M. Ohta, Y. Sugawara, and S. Morita, Jpn. J. Appl. Phys., Part 2 **34**, L1086 (1995).
[5] M. Bammerlin, R. Luthi, E. Meyer, A. Baratoff, J. Lu, M. Guggisberg, Ch. Gerber, L. Howald, and H.-J. Güntherodt, Probe Microsc. **1**, 3 (1997).
[6] R. Bennewitz, M. Bammerlin, M. Guggisberg, C. Loppacher, A. Baratoff, E. Meyer, and H.-J. Güntherodt, Surf. Sci. **438**, 289 (1999).
[7] R. Bennewitz, A. S. Foster, L. N. Kantorovich, M. Bammerlin, Ch. Loppacher, S. Schär, M. Guggisberg, E. Meyer, and A. L. Shluger, Phys. Rev. B **62**, 2074 (2000).
[8] C. Loppacher, R. Bennewitz, O. Pfeiffer, M. Guggisberg, M. Bammerlin, S. Schär, V. Barwich, A. Baratoff, and E. Meyer, Phys. Rev. B **62**, 13 674 (2000).
[9] C. Loppacher, M. Bammerlin, M. Guggisberg, S. Schär, R. Bennewitz, A. Baratoff, E. Meyer, and H.-J. Güntherodt, Phys. Rev. B **62**, 16 944 (2000).
[10] M. Guggisberg, M. Bammerlin, A. Baratoff, R. Lüthi, Ch. Loppacher, F. M. Battiston, J. Lü, R. Bennewitz, E. Meyer, and H.-J. Güntherodt, Surf. Sci. **461**, 255 (2000).
[11] R. Boisgard, D. Michel, and J. P. Aimé, Surf. Sci. **401**, 199 (1998).
[12] N. Sasaki and M. Tsukada, Jpn. J. Appl. Phys., Part 2 **37**, L533 (1998).
[13] J. P. Aimé, G. Couturier, R. Boisgard, and L. Nony, Astron. Nachr. **140**, 333 (1999).
[14] N. Sasaki and M. Tsukada, Appl. Surf. Sci. **140**, 339 (1999).

[15] J. P. Aimé, R. Boisgard, L. Nony, and G. Couturier, Phys. Rev. Lett. **82**, 3388 (1999).
[16] B. Gotsmann, C. Seidel, B. Anczykowski, and H. Fuchs, Phys. Rev. B **60**, 11 051 (1999).
[17] F. J. Giessibl, Phys. Rev. B **56**, 16 010 (1997).
[18] U. Dürig, Surf. Interface Anal. **27**, 467 (1999).
[19] U. Dürig, Appl. Phys. Lett. **75**, 433 (1999).
[20] H. Hölscher, U. D. Scharwz, and R. Wiesendanger, Appl. Surf. Sci. **140**, 344 (1999).
[21] H. Hölscher, W. Allers, U. D. Scharwz, A. Scharwz, and R. Wiesendanger, Phys. Rev. Lett. **83**, 4780 (1999).
[22] U. Dürig, Appl. Phys. Lett. **76**, 1203 (2000).
[23] U. D. Schwarz, H. Hölscher, and R. Wiesendanger, Phys. Rev. B **62**, 13 089 (2000).
[24] U. Dürig, New J. Phys. **2**, 5 (2000).
[25] Ch. Loppacher, M. Bammerlin, F. Battiston, M. Guggisberg, D. Müller, H. R. Hidber, R. Lüthi, E. Meyer, and H.-J. Güntherodt, Appl. Phys. A: Mater. Sci. Process. **66**, S215 (1998).
[26] B. Anczykowski, B. Gotsmann, H. Fuchs, J. P. Cleveland, and V. B. Elings, Appl. Surf. Sci. **140**, 376 (1999).
[27] J. Guckenheimer and P. Holmes, *Nonlinear Oscillations, Dynamical Systems, and Bifurcations of Vector Field* (Springer-Verlag, New York, 1983).
[28] J. P. Cleveland, B. Anczykowski, A. E. Schmid, and V. B. Elings, Appl. Phys. Lett. **72**, 2613 (1998).
[29] R. García and A. San Paulo, Phys. Rev. B **61**, R13 381 (2000).
[30] J. P. Aimé, R. Boisgard, L. Nony, and G. Couturier, J. Chem. Phys. **114**, 4945 (2001).
[31] R. Pérez, I. Štich, M. C. Payne, and K. Terakura, Phys. Rev. B **58**, 10 835 (1998).
[32] C. Loppacher, M. Bammerlin, M. Guggisberg, F. Battiston, R. Bennewitz, S. Rast, A. Baratoff, E. Meyer, and H.-J. Güntherodt, Jpn. J. Applied Phys. Part 2 **140**, 287 (1999).
[33] N. Sasaki and M. Tsukada, Jpn. J. Appl. Phys., Part 2 **39**, L1334 (2000).
[34] M. Gauthier and M. Tsukada, Phys. Rev. B **60**, 11 716 (1999).
[35] W. Denk and D. W. Pohl, Appl. Phys. Lett. . **59**, 2171 (1991)
[36] M. Gauthier and M. Tsukada, Phys. Rev. Lett. **85**, 5348 (2000).
[37] L. N. Kantorovich, J. Phys.: Condens. Matter **13**, 945 (2001).
[38] M. Gauthier and M. Tsukada (unpublished).